Biochimica et Biophysica Acta 893 (1987) 452–469
Elsevier

BBA 42611

Optical characterization of intermediates in the water-splitting enzyme system of photosynthesis – possible states and configurations of manganese and water

Ö. Saygin * and H.T. Witt

Max-Volmer-Institut für Biophysikalische und Physikalische Chemie, Technische Universität Berlin, Berlin (Germany)

(Received 1 April 1987)

Key words: Photosynthesis; Water splitting; Manganese; Spectroscopy; S-state transition; (*Cyanobacterium*)

Absorption changes coupled with the individual transitions S_0–S_3 and redox reactions in the water-splitting enzyme system S of photosynthesis have been measured. The principal difficulties of measuring the very small absorption changes in the ultraviolet coupled with those reactions have been reduced drastically through the use of a highly purified Photosystem II complex isolated from the *Cyanobacterium synechococcus*. The general problem caused by the mixing of the S states during a train of flashes and the falsification through the overlap with absorption changes of Q_B (binary oscillations) have been treated as follows. (1) The binary oscillations were bypassed through the use of silicomolybdate and high concentrations of DCBQ, respectively, as external electron acceptor. (2) Stable absorption changes of the mixed S-state transitions have been deconvoluted through fitting procedures to get the changes of the individual transitions of $S_1 \rightarrow S_2 \rightarrow S_3 \rightarrow S_0 \rightarrow S_1$. (3) Kinetically resolved absorption changes of the S-states in the 100-μs range gave independent information on the individual transitions. (4) Stable absorption changes of the $S_0 \rightarrow S_1$ transitions in the forefront were induced after shifting the S states through low concentrations of NH_2OH two units backwards. Analysis of the resulting sequence $S_x \rightarrow S_0 \rightarrow S_1 \rightarrow S_2 \rightarrow S_3 \rightarrow S_0$, beginning with an NH_2OH depending pre-state, S_x, and followed by an $S_0 \rightarrow S_1$ transition not mixed with the opposite $S_3 \rightarrow S_0$ transition, increased the conclusiveness considerably. It results that the ultraviolet spectrum of the $S_0 \rightarrow S_1$ transition is different from the spectra of the $S_1 \rightarrow S_2$ and $S_2 \rightarrow S_3$ transition. Possible states of manganese, water and surplus charges responsible for these spectra are presented.

Introduction

One fundamental reaction in photosynthesis, the splitting of water, takes place in System II of photosynthesis. This process is started by the photooxidation of chlorophyll a_{II} (P-680) [1,2]. The ejected electron is trapped by the first stable acceptor, a plastoquinone molecule, Q_A (X-320) [3,4]. This charge separation is vectorial and sets up an electric field across the center [5,6]. From Q_A^- the electron is transferred via Q_B [7] through a pool of plastoquinones, Q, lastly to System I where

* Present address: Institute of Environmental Sciences, Bogazici University, Bebek, Istanbul, Turkey.

Abbreviations: Chl *a*, chlorophyll *a*; Chl a_{II}, P-680 = photoactive chlorophyll in Photosystem II; Q_A, primary quinone acceptor of Photosystem II; PS I, Photosystem I; PS II,Photosystem II; D_1, immediate donor to Chl a_{II}^+; D_2, donor characterized by EPR signal II_{vf}; DCBQ, 2,5-dichloro-*p*-benzoquinone; Mes, 4-morpholineethanesulphonic acid; DCMU, 3-(3′,4′-dichlorophenyl)-1,1-dimethylurea; SiMo, silicomolybdate.

Correspondence: H.T. Witt, Max-Volmer-Institut für Biophysikalische und Physikalische Chemie, Technische Universität Berlin, Sekr. PC 14, Strasse des 17. Juni 135, D-1000 Berlin 12, Germany.

excited Chl a_I (P-700) [8] transfers the electron to the terminal acceptor, $NADP^+$. The Q-pool spans the membrane from the outside of System II towards the inside of system I [9].

The oxidized Chl a_{II} extracts electrons from water via possibly two electron carriers, D_1 [10] and D_2 [11] and is thereby re-reduced. In order to use the univalent oxidizing power of Chl a_{II} for the cleavage of 2 H_2O into 4 H^+, 4 e^- and for the evolution of one O_2, four Chl a_{II} oxidations have to cooperate to supply water with the necessary four oxidizing equivalents. First, in three Chl a_{II} turnovers, three electrons are sequentially extracted step-by-step from a water-splitting manganese-containing enzyme system S. The three oxidizing equivalents thereby generated are stabilized and stored. After a fourth photooxidation of Chl a_{II} and electron extraction, the formation of a further oxidizing equivalent takes place, followed by the evolution of one O_2 [12]. According to Kok [13] the four unknown oxidation states of S are termed S states. (The indices n indicate the number of electrons extracted.) The reaction cycle starts in S_0. The states S_0, S_1, S_2 and S_3 are stable with lifetimes ranging from seconds to several minutes. S_3 is followed by an unstable S_4 state which reverts to S_0 within 1 ms, together with the O_2 evolution from water. In the dark-adapted system the major state is S_1. Therefore, under these conditions, the reaction starts with S_1 and the sequence is

$$S_1 \rightarrow S_2 \rightarrow S_3 \xrightarrow{(S_4)} \begin{matrix} \nearrow O_2 \\ \rightarrow \end{matrix} S_0 \rightarrow S_1 \qquad (1)$$

i.e., O_2 evolution takes place after the third flash [12]. It is the goal of this work to evaluate absorption changes of the different S-state transitions in order to get information on the chemical meaning of those states and on the mechanism of water oxidation. The stability of the attained S_n states as well as the characteristic period-four oscillations allow one to distinguish absorption changes of S from non-oscillatory and/or transient absorption changes originating from other events. Reversible redox reactions of the one-electron carriers, Chl a_{II}, Q_A, the D donors and others are eliminated if measurements are performed, e.g., 0.5 s after flash excitation. However, three complications have to be considered.

Principal problems

Binary oscillations. In contrast to Q_A, the subsequent electron carrier, Q_B, has a two-electron capacity. Q_B^- is stable until, upon a second Chl a_{II} photooxidation, two electrons are accumulated as Q_B^{2-} and released into the PQ-pool; i.e., Q_B^- is formed in the first and odd flashes, Q_B^{2-} in even flashes. This Q_B^- oscillates with a periodicity of two [7] and interferes with the quaternary oscillation of the S states.

Mixing of the S states. If only the S_1 state is present after dark adaptation and if each flash transfers one state into exactly one higher state, then the correlation of measured absorption changes with the different S_n states could be unambiguous. However, (a) the predominant state after dark adaptation is S_1, but not exclusively, an unknown remainder is in S_0; (b) some centers where no charge separation by the flash light takes place cause 'misses' (probability = α), retarding the S-state progression; (c) 'double hits' (probability = β), mainly due to excitation by the measuring beam, cause more than one turnover, advancing the S-state progression. For these reasons the populations of the S-state transitions are increasingly mixed with progressive flash numbers. (After many flashes the states are even randomized so that after each flash 25% of each transition takes place simultaneously.) The mixing is also responsible for the fact that O_2 evolution takes place not only after the 3rd and 7th flash, but also, to a smaller extent, more or less after each other flash [12]. From such a pattern of O_2 evolution the values of S_0/S_1 after dark adaptation and of α and β can be estimated (see below) [13].

First flash event. Irreversible absorption changes occurring only once after the first flash may disturb the first period of oscillation. Such absorption changes may be due to inactive particles ready for only one electron transfer.

Types of correction

(i) Binary oscillations have been usually eliminated through subtraction of their contributions from the overall oscillation. However, precise information on the extent of these contributions from such binary oscillation as a function of flash number is rarely available. This may lead to considerable mistakes.

(ii) To draw conclusions on the absorption changes belonging to one individual S-state transition, one has to deconvolute the mixed S-state transitions through calculations. Such corrections are based on the parameters of misses, α, double hits, β, and the initial S_0/S_1 ratio in the dark-adapted state. But, we have shown in Ref. 20 that one may obtain different sets of individual absorption changes by variations of the values of the parameters within discernable accuracy. Therefore, such procedures do not permit an unambiguous determination of the absorption changes coupled with the individual unmixed S-state transitions.

(iii) The first flash problem is often bypassed by skipping the absorption changes after the first flash in the calculations. Since the first transition is least mixed with other transitions, this results in a significant loss of information.

Existing results

Using such corrections attempts considering the patterns of absorption changes of S in the ultraviolet were done by Velthuys [14] who concluded from his measurements a pattern of $0:+1:0:-1$ for the absorption changes accompanying the transitions $S_0 \rightarrow S_1 \rightarrow S_2 \rightarrow S_3 \rightarrow S_0$. This was further confirmed by Lavergne [15]. According to this result, $S_0 \rightarrow S_1$ and $S_2 \rightarrow S_3$ transitions should be coupled with an accumulation of redox equivalents that are not visible in the studied ultraviolet region. This may be explained by the formation of colorless oxidation products of water in the $S_0 \rightarrow S_1$ and $S_2 \rightarrow S_3$ transitions. Later, Renger and Weiss [16,17] reported two interfering patterns, $0:2:0:-2$ for one species and $1:-1:+1:-1$ for another. However, the spectra published in [16,17] were superimposed by a contribution from the binary oscillations located at the acceptor side (private communication by Renger), so that the outlined interpretations are therefore no longer relevant [18]. Dekker et al [19] proposed a pattern of $+1:+1:+1:-3$ for absorption changes in the ultraviolet region accompanying the transitions $S_0 \rightarrow S_1 \rightarrow S_3 \rightarrow S_3 \rightarrow S_0$. They suggested that three $Mn^{3+} \rightarrow Mn^{4+}$ transitions take place which are reversed in the last step. The discrepancies between the patterns of the four authors may be mainly due to differences in the use of the necessary corrections rather than due to differences in experimental results. For clarification of the discrepancies we introduced additional independent methods. The results we obtained in Ref. 20 at one special wavelength (384 nm) provided the information that all three transitions, $S_0 \rightarrow S_1$, $S_1 \rightarrow S_2$ and $S_2 \rightarrow S_3$, are coupled with absorption changes contrasting Lavergne and Velthuys but being in accordance with Dekker et al. However, the question whether all three transitions are equal and have the same behavior at different wavelengths has not been answered in Ref. 20. Using the approaches outlined below, we shall report in this work that the transitions $S_1 \rightarrow S_2$ and $S_2 \rightarrow S_3$ are coupled with similar spectra of absorption changes but that the $S_0 \rightarrow S_1$ transition exhibits a different spectrum. The consequences regarding the possible states of manganese and water are discussed. A short note is published in Ref. 21.

Methods

Approaches

For the elimination of the binary oscillations of Q_B^- from the acceptor side we used three different methods. (a) We used SiMo as external acceptor in the presence of DCMU which eliminates binary oscillations from the acceptor side by extracting electrons directly from Q_A, bypassing and preventing the Q_B action. This method is the safest way for making measurements without disturbance through Q_B oscillations and is therefore always used as a check when also methods (b) and (c) are used. The problem with silicomolybdate is that this substance absorbs much light especially in the ultraviolet region. This makes the measurements difficult. To overcome this complication, we have alternatively eliminated the binary oscillations as follows. (b) We used DCBQ as external acceptor but increased its concentration to $6 \cdot 10^{-4}$ M which is 6-times higher than that used by Dekker et al [19]. Only under such high concentration of DCBQ were the obtained patterns identical to those obtained with silicomolybdate and DCMU. This method yielded especially good results in the wavelength range of 340–370 nm where Q_B^- has a small amplitude anyhow. This can be explained by considering that the actual time-determining step in the electron chain is the

electron transport to the external acceptor. Increasing its concentration on the other hand helps to extract the electrons from Q_B^- directly to the external acceptor during the time of 0.5 s between the flashes [22]. (c) By using no external acceptor at all we observed in the above ultraviolet region (340–370 nm) the same pattern as with silicomolybdate. The disappearance of the binary oscillations in this case is due to the fact that in a dark-adapted preparation in the absence of any oxidizing agents (like that of an external acceptor) the Q_B^-/Q_B ratio is close to one. Therefore only that portion of Q_B which deviates from this ratio can lead to oscillation [23]. However, Q_B/Q_B^- absorption change at this wavelength region is small compared to manganese absorption changes [24]. This means that the binary oscillations become negligible. Since the electron capacity of the Q pool is limited, in this case the total amplitude of the signals decreases monotonically with increasing number of flashes. All three methods allowed measurement of the quaternary oscillations of S directly; i.e., without an overlap of binary oscillation and without the need for subtractions which are always a source of mistakes (see above).

Apart from the normal conditions, we performed additional experiments with low concentrations (24 μM) of hydroxylamine (NH_2OH) which shifts the S states backwards by two units to an unknown state, S_x [25]. Under these conditions, after dark adaptation, O_2 is evolved in the fifth flash, i.e., instead of $S_1 \rightarrow S_2 \rightarrow S_3 \rightarrow S_0 \rightarrow S_1$ the following transition takes place:

$$S_x \rightarrow S_0 \rightarrow S_1 \rightarrow S_2 \rightarrow S_3 \xrightarrow{(S_4)} \overset{O_2}{\nearrow} \rightarrow S_0 \qquad (2)$$

This has an enormous advantage: one critical point in the transition under normal conditions is the transition in the fourth flash, $S_0 \rightarrow S_1$; i.e., the last step of the quaternary period (see Eqn. 1). This transition is most heavily mixed with simultaneous transitions from $S_3 \rightarrow S_0$ (20–45%). The absorption changes coupled with the $S_3 \rightarrow S_0$ transition may be up to 3-times larger than those of the other transitions and have a sign opposite to the other transitions. This situation is avoided, however, when it becomes possible to observe with NH_2OH the $S_0 \rightarrow S_1$ transition at the beginning of the flash series, when the mixing is small and when also the other transitions, $S_1 \rightarrow S_2$ and $S_2 \rightarrow S_3$, can be observed before the opposing jump, $S_3 \rightarrow S_0$. In this way one obtains, in addition to the information without NH_2OH, an independent set of absorption changes reducing the source of mistakes considerably.

Materials

Oxygen-evolving PS II particles from thermophilic cyanobacteria *Synechococcus* sp. were separated according to Ref. 26 and subsequently highly purified [27]. In single turnover flashes, the resulting PS II complexes evolved 1/4 O_2 per 50 chlorophylls on the average. This corresponds to more than approx. 3000 μmol O_2/mg Chl per h in saturating permanent light. The suspensions used for measurements contained $3 \cdot 10^{-8}$ M Chl a_{II} centers, 0.01 M $MgCl_2$, 0.5 M mannitol, $2 \cdot 10^{-2}$ M Mes/NaOH (pH 7.0). As external acceptor we used $2 \cdot 10^{-5}$ M silicomolybdate or in kinetic experiments $6 \cdot 10^{-4}$ M DCBQ or no acceptor at all. The temperature was 20 °C.

The PS II particles were dark-adapted at least for 1 h before the measurements. Every 0.5 s after each flash, the absorption of the solution was measured for a few milliseconds. In the experiments with hydroxylamine the PS II particles were incubated after dark adaptation with 24 μM hydroxylamine for 20 min in the absence of an acceptor. After this incubation time silicomolybdate was added ($2 \cdot 10^{-5}$ M) and the measurements were started 1 min later. Under these conditions about 25% of the particles were inactive in oxygen evolution. Optical changes were measured with the same apparatus as described in Ref. 28 except that below 330 nm a high-pressure mercury lamp (Hannovia 250 W) was used as the light source.

In each flash, the reduction of the electron acceptor takes place accompanied by absorption changes. The extent – in the order of up to $\Delta\epsilon \approx 1$ $mM^{-1} \cdot cm^{-1}$ – and the sign of the changes depend on the acceptor type and are a function of the wavelength. Such changes are the same in each flash and are superimposed as a nonoscillating constant step to the oscillating stable levels of absorption changes of S. This results in a shift of

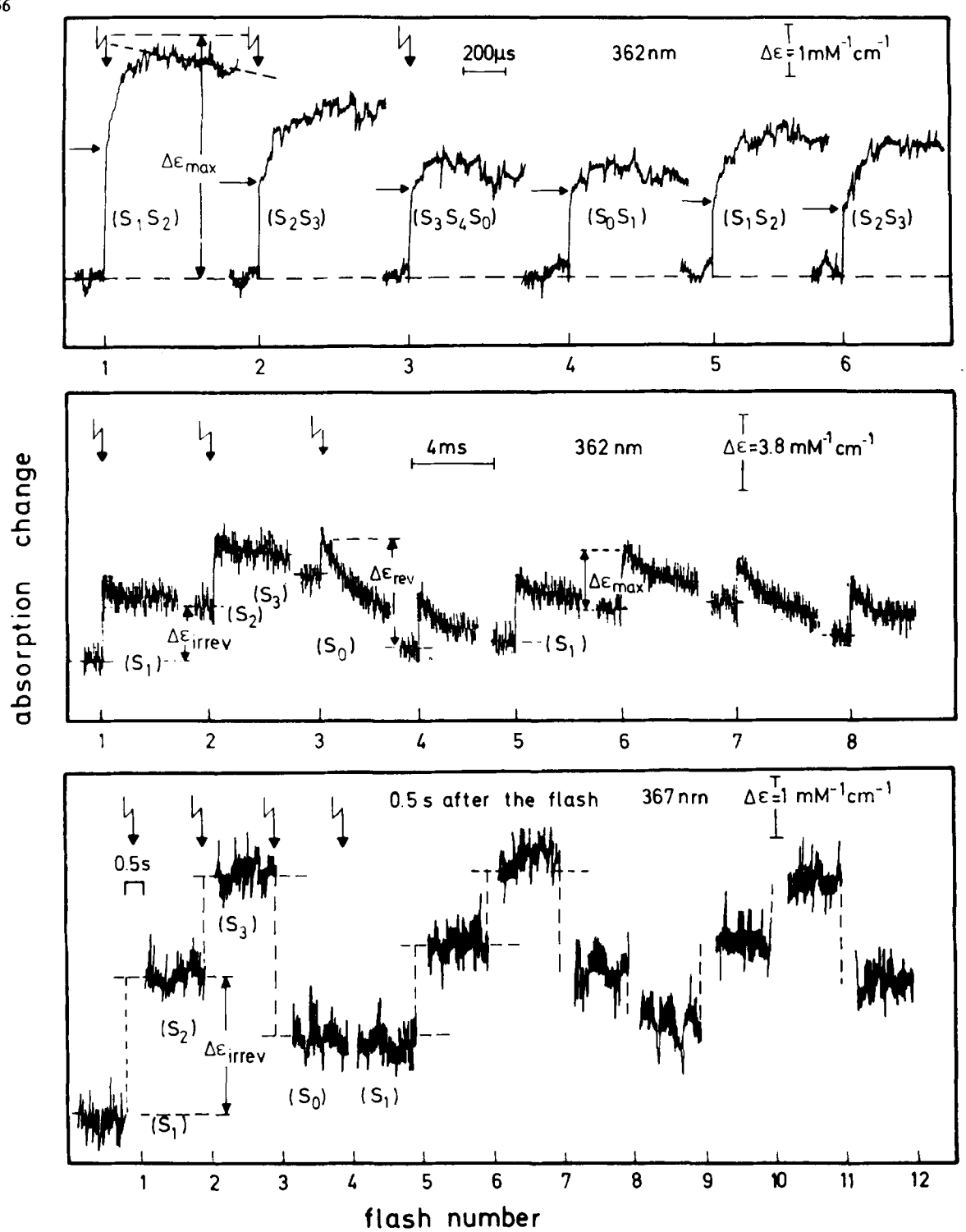

Fig. 1. Time-course of absorption changes of dark-adapted isolated PS II complexes from *Synechococcus* as a function of the flash number. Dark time between the flashes, 0.5 s. Concentration of the reaction centers, $3 \cdot 10^{-8}$ M. Top: absorption changes at 362 nm in the 200 µs time range in the absence of an external acceptor. For comparison the level of the absorptions before the flashes is moved to the same position. The pattern is the average of 12 measurements. Center: absorption changes at 362 nm in the 4-ms time range with 0.6 mM DCBQ as acceptor. The pattern is the average of two measurements. Below: stable levels of absorption changes at 367 nm 0.5 s after each flash. Acceptor $2 \cdot 10^{-5}$ M silicomolybdate. The pattern is the average of 14 measurements.

the stable levels proportional to the flash number. In all figures constant contributions causing such shifts have been subtracted.

Results

The characteristic changes of $\Delta\epsilon_{max}$, $\Delta\epsilon_{rev}$ *and* $\Delta\epsilon_{irrev}$

Fig. 1, bottom, shows a typical pattern of stable absorption changes of the enzyme system S as the 'end product' of a chain of preceding reactions, triggered by the electron extraction through Chl a_{II}^{+}. The main feature of such a pattern are oscillating damped quaternary absorption changes. The damping of the oscillation is due to the increased mixing of the different S_n states with increasing flash numbers. Usually, other workers in this field do not consider the changes after the first flash, since in their experimental results these absorption changes deviate considerably from the expected values (compared with flash numbers 5, 9, etc.) due to unknown effects after dark adaptation. In our measurements with SiMo at 367 nm (Fig. 1, bottom), the effect after the first flash is not significantly different from the corresponding effect of the 5th and 9th flash. Therefore, the absorption changes of all four flashes in the first

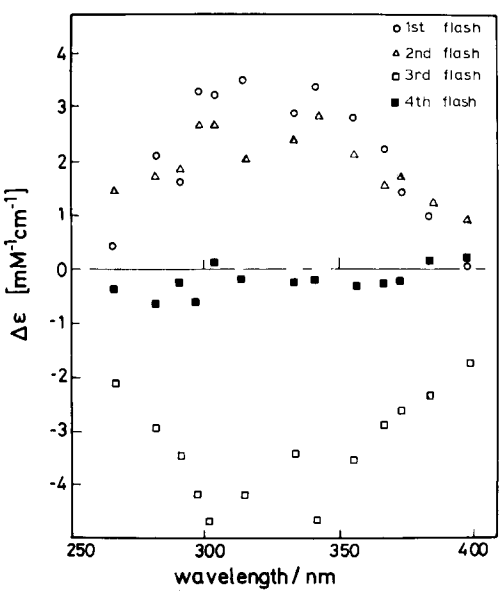

Fig. 2. Stable levels of absorption changes 0.5 s after the flash (see Fig. 1, below) in dependence on the wavelength and as a function of the first four flashes. Concentration of the reaction centers, $3 \cdot 10^{-8}$ M. Acceptor silicomolybdate, $2 \cdot 10^{-5}$ M.

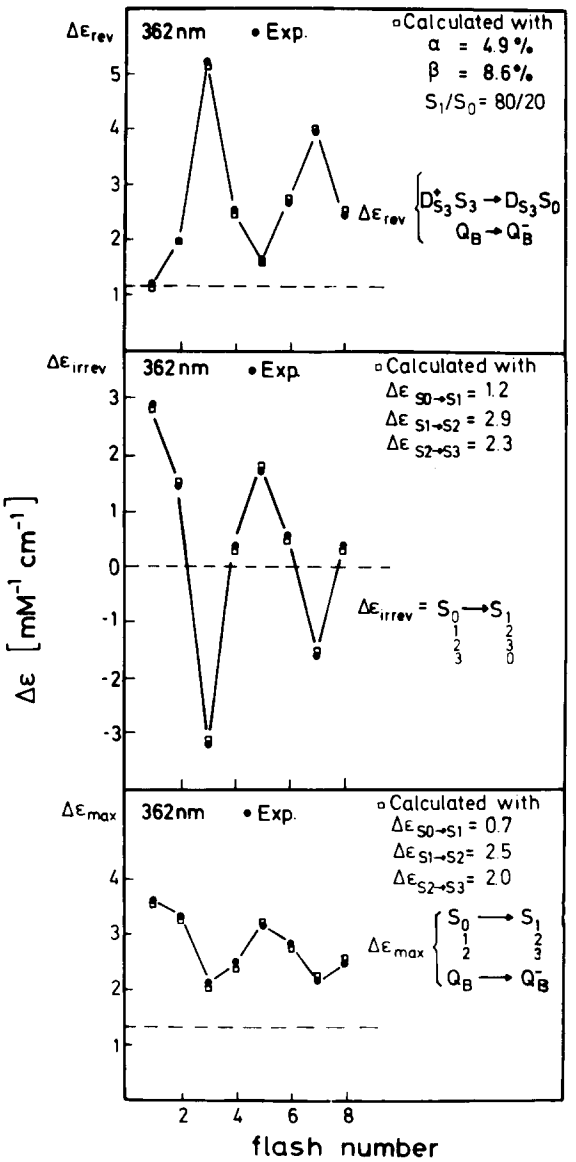

Fig. 3. Molar extinction coefficient changes, $\Delta\epsilon_{rev}$, $\Delta\epsilon_{irrev}$ and $\Delta\epsilon_{max}$ corresponding to Fig. 1, center, as a function of the flash number. Measured values: full circles; calculated values; open squares. Top: the oscillation of $\Delta\epsilon_{rev}$ corresponds to the O_2 evolution (see text). From the fitting procedure one gets the outlined parameters α, β, and S_1/S_0 responsible for the mixing of the S states. Center and below: with the parameters of the mixing the uncorrected measured $\Delta\epsilon_{irrev}$ values and $\Delta\epsilon_{max}$ (full circles) can be fitted (open squares), if one uses for the individual unmixed $\Delta\epsilon_{S_n \rightarrow S_{n+1}}$ values those that our outlined in the figures, top right.

period are shown in Fig. 2 as a function of wavelength. The spectra after the 1st and 2nd flash, mainly due to $S_1 \rightarrow S_2$ and $S_2 \rightarrow S_3$ transitions, respectively, are similar. The spectra are, however, mixed with other transitions due to misses, α, and double hits, β. The spectrum after the 4th flash, which should furnish information on the $S_0 \rightarrow S_1$ transition, is nearly zero through mixing of changes coupled mainly with the opposite transition, $S_3 \rightarrow S_0$. (All authors in this field are measuring after the 4th flash practically no stable absorption changes in the whole ultraviolet region.) The 'true spectra' of the $S_n \rightarrow S_{n+1}$ transition, especially that of $S_0 \rightarrow S_1$, can therefore only be evaluated by deconvolution of the mixing.

Deconvolution requires information about the misses, α, double hits, β, and the initial S_0/S_1 ratio available directly from the pattern of O_2 evolution (see Introduction). They can be obtained from the absorption changes of $S_3 \rightarrow S_0$ transitions which are coupled with O_2 evolution. Before going into detail, the meaning of the different phases of the kinetics, e.g., at 362 nm with DCBQ as acceptor are discussed first. In general, six partial reactions are induced by the absorption of 1 $h\nu$ per reaction center II (see Fig. 1 and Scheme I):

$$Q_A + \text{Chl } a_{II} \xrightarrow{h\nu} \text{Chl } a_{II}^+ + Q_A^-$$

$$\text{Chl } a_{II}^+ + D \rightarrow \text{Chl } a_{II} + D^+$$

$$D_{S_n}^+ + S_n \rightarrow D_{S_n} + S_{n+1} \quad n = 0, 1, 2$$

$$D_{S_3}^+ + S_3 \rightarrow D_{S_3} + S_0$$

$$Q_A^- + Q_B \rightarrow Q_A + Q_B^-$$

$$Q_B^- + \text{acceptor}_{ox} \rightarrow Q_B + \text{acceptor}_{red}$$

(i) The fast rise in up to 1 μs up to the horizontal arrow (Fig. 1, top and Scheme I) is set up by the Q_A reduction and oxidation of the terminal donor D (the oxidation and reduction of Chl a_{II} and that of its immediate donor [10] take place in the nanosecond range and do not appear). (ii) In the subsequent rise within 200 μs (Fig. 1, top and Scheme I) D^+ oxidizes S_n to S_{n+1} ($n = 0, 1, 2$) (see Table II, below). Only that portion of D^+ is not reduced which transfers later in the decay phase S_3 to S_0. This portion is indicated as D_{S_3}. In the case of DCBQ as acceptor, the electron moves from

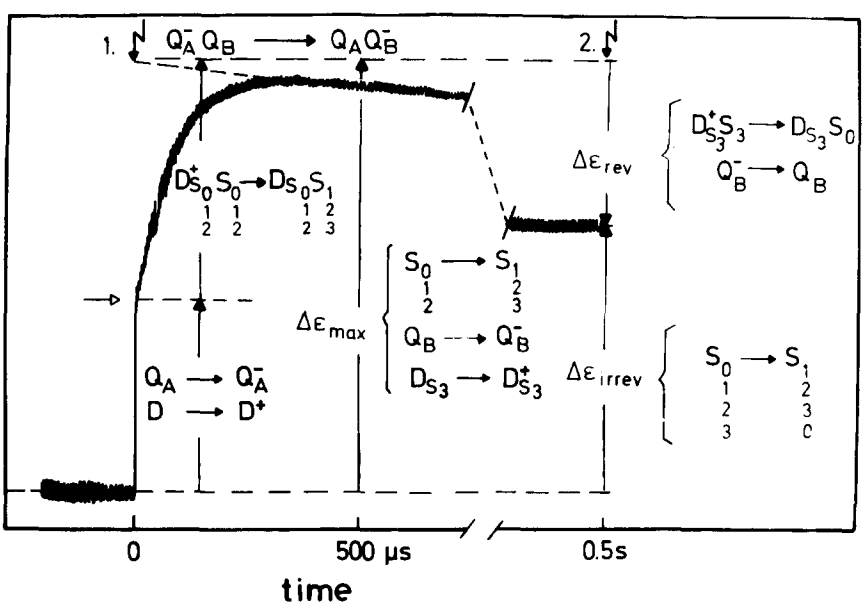

Scheme I. Schematic representation of the time-course of absorption changes and $\Delta\varepsilon$, coupled with the different redox reactions at 360 nm. $\Delta\varepsilon_{D/D^+}$ as well as $\Delta\varepsilon_{Q_A^- Q_B / Q_A Q_B^-}$ are practically zero. Contributions due to the external acceptor reduction are subtracted (for details, see text).

Q_A^- to Q_B which is practically not coupled with any absorption changes at 360 nm [24]. The total rise is indicated as $\Delta\epsilon_{max}$. (iii) The phase which decays thereafter in about 1 ms indicate especially $D_{S_3}^+ + S_3 + \text{water} \xrightarrow{(S_4)} D_{S_3} + S_0 + O_2$. This transfer takes place more or less after all flashes; the maximum decay appears after the 3rd and 7th flash (Fig. 1, center). The further decay up to 0.5 s to the stable levels (see Fig. 1, center and bottom) is due to the oxidation of Q_B^- by the external acceptor A (in the case of A = SiMo, this acceptor bypasses Q_B and the decay is due to oxidation of Q_A^- by SiMo). The total decay phase is indicated as $\Delta\epsilon_{rev}$ (see Fig. 1, center, and Scheme I).

Since within 0.5 s deactivation of S_1, S_2 and S_3 is negligible, the difference of the level after 0.5 s and the level before the flash, indicates the absorption change of $S_n \rightarrow S_{n+1}$ and $S_3 \rightarrow S_0$ together with that of the acceptor reduction. The change through the acceptor, A, is the same in each flash and has been subtracted (see Materials). Therefore, the difference between the levels after 0.5 s and the level before the flash, i.e., $\Delta\epsilon_{irrev}$ indicates the absorption change of the transition $S_n \rightarrow S_{n+1}$ and $S_3 \rightarrow S_0$.

Deconvolution procedure – $\Delta\epsilon_{rev}$, $\Delta\epsilon_{irrev}$

The total $\Delta\epsilon_{rev}$ decay of Fig. 1, center, is depicted in Fig. 3, top, as a function of the flash number. $\Delta\epsilon_{rev}$ is composed of the millisecond amplitude due to the transition $D_{S_3}^+ S_3 \rightarrow D_{S_3} S_0$ and – if DCBQ is the acceptor – due to $Q_B^- \rightarrow Q_B$, which is the same in each flash. The dashed offset in Fig. 3, top, includes the constant change of $Q_B^- \rightarrow Q_B$. As the absorption changes of D [29–31] are practically zero at 362 nm, the oscillating amplitudes above the onset are due to the contribution of $S_3 \rightarrow S_0$ in each flash. These amplitudes are proportional to the extent of O_2 evolution. The pattern of O_2 evolution depends on the parameters α, β and S_0/S_1. To fit these oscillations in Fig. 3, top (closed circles), one has to use those values of the parameters α, β and initial S_0/S_1 ratio which are listed in Fig. 3, top, right. The amplitudes calculated from these values are indicated by open squares. With these parameters one can analyze the pattern of the stable levels of absorption changes, $\Delta\epsilon_{irrev}$ of Fig. 1, center. $\Delta\epsilon_{irrev}$ is redrawn in Fig. 3, center (closed circles). $\Delta\epsilon_{irrev}$ represents the uncorrected, i.e., mixed $S_n \rightarrow S_{n+1}$ and $S_3 \rightarrow S_0$ transitions. The best fit is obtained when for the corrected, i.e., unmixed transitions the following $\Delta\epsilon$ values are used: for the $S_0 \rightarrow S_1$ transition $\Delta\epsilon = 1.2$, for $S_1 \rightarrow S_2$ $\Delta\epsilon = 2.9$ and for $S_2 \rightarrow S_3$ $\Delta\epsilon = 2.3$ $mM^{-1} \cdot cm^{-1}$ (Fig. 3, center, open squares). The $S_0 \rightarrow S_1$ transition at 362 nm is much smaller than the $S_1 \rightarrow S_2$ and $S_2 \rightarrow S_3$ transitions. Eight further patterns (not shown, but similar to the one in Fig. 1, center) were analyzed with regard to $\Delta\epsilon_{irrev}$ by the same method. The average resulting from these fittings is presented in Table I. Without considering the values of the fitting procedures incontestable (see Introduction), we can at least say that the $S_0 \rightarrow S_1$ transition at 362 nm is coupled with a much smaller absorption change compared to the other two transitions, $S_1 \rightarrow S_2$ and $S_2 \rightarrow S_3$. Up to this point, we used the same method as other authors in this field, but with the exception that binary oscillation caused by Q_B has been eliminated by using DCBQ in very high concentration, which was checked by comparison with addition of SiMo (see Methods).

Analysis of the kinetics – $\Delta\epsilon_{max}$

Independent information concerning the absorption changes of the individual S-state transitions is available from the inspection of their oxidation kinetics in the 200 μs range (Fig. 1, top). We focused our attention again on 362 nm. The fast rise less than approx. 1 μs up to the arrow indicates the $D \rightarrow D^+, Q_A \rightarrow Q_A^-$ transfer (see Scheme I). Since the experiments were performed without any external acceptor, the extent of the rise (less than approx. 1 μs) in Fig. 1, top, decreases with increasing flash number because the Q pool is gradually reduced (s. arrows). The use of SiMo is not necessary, because under these conditions binary oscillations do not occur (see Methods). The subsequent rise within 200 μs is due to $D_n^+ S_n \rightarrow D_n S_{n+1}$ (see Scheme I). Since at 362 nm the absorption changes of D are practically zero, the half-rise times of the absorption changes beginning at the point of the arrows indicate the $S_n \rightarrow S_{n+1}$ transition times. The amplitude of this phase are the absorption changes coupled with the $S_n \rightarrow S_{n+1}$ transition. The half-life times have been evaluated for the different flash numbers and are shown in Table II. The values represent, besides

TABLE I

CHANGES OF THE MOLAR EXTINCTION COEFFICIENTS OF THE UNMIXED INDIVIDUAL S-STATE TRANSITIONS AT 362 nm

The values were evaluated from $\Delta\epsilon_{irrev}$ and $\Delta\epsilon_{max}$ (see text). Eight time-resolved patterns corresponding to the pattern in Fig. 1, center, were analyzed and averaged.

	$\Delta\epsilon_{362}$ ($M^{-1}\cdot cm^{-1}$)	
	evaluated from $\Delta\epsilon_{irrev}$	evaluated from $\Delta\epsilon_{max}$
$S_0 \rightarrow S_1$	770	480
$S_1 \rightarrow S_2$	2770	2630
$S_2 \rightarrow S_3$	2760	2490

the transition times, also the times for re-reduction of D^+ and oxidation of the S_n states, respectively. With regard to the time range, the kinetics correspond to those obtained in Ref. 32 and 16. However, the individual time constants are different up to a factor of 5. The slowest oxidation of S_n to S_{n+1} (not $S_3 \rightarrow S_0$) has a half-life time of about 100 μs which is at least 15-times faster than the other processes with an opposing absorption change like the $S_3 \rightarrow S_0$ transition as well as the acceptor reduction taking place in the millisecond range. Therefore, the maximal amplitudes of the rise above the arrows indicate the $S_n \rightarrow S_{n+1}$ transition. These transitions – including the $S_0 \rightarrow S_1$ transition – are not mixed with the opposite $S_3 \rightarrow S_0$ transition taking place 15-times later. Already by simple inspection one can see in Fig. 1, top (no acceptor) that $\Delta\epsilon_{max}$ minus the fast change less than approx. 1 μs indicated by arrows shows at 362 nm a nearly equal amplitude after the 1st and 2nd flash ($S_1 \rightarrow S_2$ and $S_2 \rightarrow S_3$) while after the 4th flash ($S_0 \rightarrow S_1$) it is much smaller. We further analyzed $\Delta\epsilon_{max}$ quantitatively for the pattern in Fig. 1, center (acceptor DCBQ).

TABLE II

HALF-LIFE TIMES OF THE ELECTRON TRANSFERS DURING THE S-STATE TRANSITIONS

The indicated times were obtained from experiments in the absence of an external acceptor at 362 nm. The values are taken from patterns corresponding to Fig. 1, top. At pH 5.5 a significant change of the half-life time was only observed for the $S_2 \rightarrow S_3$ transition.

	$S_0 \xrightarrow[-e^-]{} S_1 \xrightarrow[-e^-]{} S_2 \xrightarrow[-e^-]{} S_3 \xrightarrow[-e^-]{(S_4)} S_0$			
pH 6.5	50 μs	40 μs	100 μs	1.5 ms
pH 5.5			220 μs	

The $\Delta\epsilon_{max}$ values are depicted in Fig. 3, bottom (solid circles). The dashed offset includes the constant change of the $Q_B \rightarrow Q_B^-$ transfer. Using the same values of parameters (misses, α, double hits, β, and initial S_0/S_1 ratio) evaluated from $\Delta\epsilon_{rev}$ (Fig. 3, top), the best fit is obtained for the corrected, i.e., unmixed transitions, if the following $\Delta\epsilon$ values are used (Fig. 3, bottom, open circles):

$S_0 \rightarrow S_1$: $\Delta\epsilon = 675$; $S_1 \rightarrow S_2$: $\Delta\epsilon = 2540$;

$S_2 \rightarrow S_3$: $\Delta\epsilon = 2010\ M^{-1}\cdot cm^{-1}$

The $S_0 \rightarrow S_1$ transition at 362 nm showed again a smaller absorption change than the $S_1 \rightarrow S_2$ and $S_2 \rightarrow S_3$ transitions. Eight other patterns (not shown, but similar to those of Fig. 1, center) were analyzed with regard to $\Delta\epsilon_{max}$. The obtained averages are depicted in Table I. One can see that both methods, i.e., evaluation of $\Delta\epsilon$ from $\Delta\epsilon_{irrev}$ and $\Delta\epsilon_{max}$, respectively, yield similar results: $S_0 \rightarrow S_1$ has a much smaller $\Delta\epsilon_{362nm}$ value than the other two transitions ($S_1 \rightarrow S_2$; $S_2 \rightarrow S_3$). The latter two have almost the same value.

Backwards shift of two S units through the action of NH_2OH

Despite the similarities in the results of two independent methods ($\Delta\epsilon_{irrev}$ and $\Delta\epsilon_{max}$) we searched for independent sets of experiments in order to arrive at an unambiguous decision. For this reason, in the following we have additionally analyzed the irreversible absorption changes, $\Delta\epsilon_{irrev}$, 0.5 s after the flash in the presence of low non-destructive concentrations of NH_2OH which shift the oscillation pattern backwards by two units [25].

Although the true mechanism of the two-unit backward shift through NH_2OH and the transition by the first flash, respectively, is not yet known (but see Discussion), it is accepted that during the 2nd, 3rd and 4th flash mainly transitions $S_0 \rightarrow S_1$, $S_1 \rightarrow S_2$, and $S_2 \rightarrow S_3$, respectively, occur. This means that the $S_0 \rightarrow S_1$ transition is shifted by NH_2OH from the 4th flash to the 2nd flash which has the advantage of being practically unmixed with the $S_3 \rightarrow S_0$ transition. By measuring

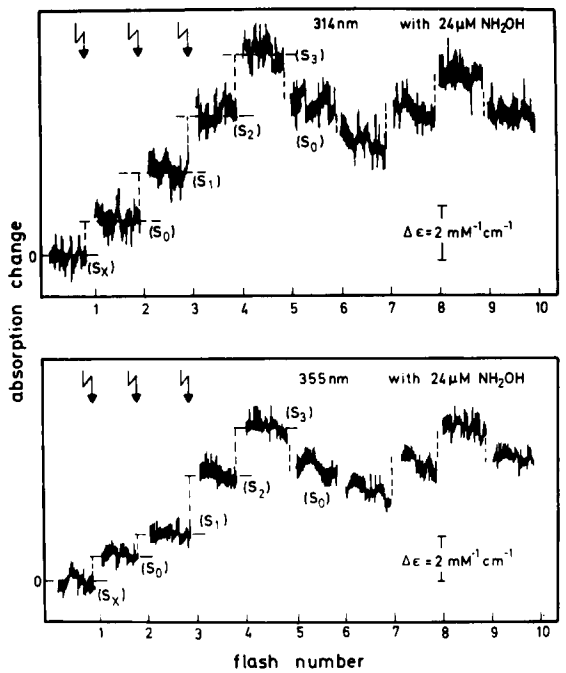

Fig. 4. Stable levels of absorption changes of dark-adapted PS II particles 0.5 s after the flash at 314 nm and 355 nm in the presence of 24 μM hydroxylamine (NH_2OH) as a function of the flash number. Concentration of reaction centers $3 \cdot 10^{-8}$ M. After incubation with 24 μM NH_2OH for 20 min in the dark, silicomolybdate was added ($2 \cdot 10^{-5}$ M). The measurements were done 1 min later. The pattern at 314 nm is the average of 20 and that at 355 nm the average of 24 measurements. The backward shift of two flash units is evident by comparison, e.g., of the $S_3 \rightarrow S_0$ transition in this figure and that in Fig. 1, bottom, without NH_2OH.

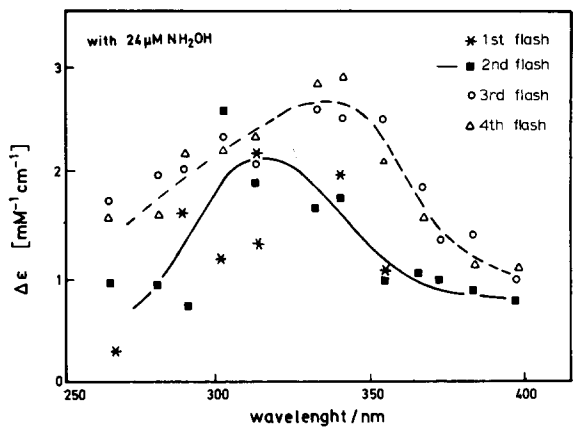

Fig. 5. Spectra of the stable levels of absorption changes of the first four flashes in the presence of 24 μM hydroxylamine. Other details, see Fig. 4.

the patterns in the presence of hydroxylamine as a function of wavelength and subtracting again a linear drift due to SiMo reduction, we observed two different types of patterns in the ultraviolet region. Fig. 4, top and bottom, shows typical examples at 314 and 355 nm. One can easily recognize in both cases the backward shift by two units: the $S_3 \rightarrow S_0$ transition, for instance, takes place after the 5th flash instead of the 3rd flash without NH_2OH (see Fig. 1, bottom). While at 314 nm the amplitudes of the stable absorption changes after the 2nd, 3rd and 4th flash are similar, at 355 nm the jump after the 1st and 2nd flash is much smaller than those after the 3rd and 4th flash. The spectrum of the absorption changes in the 2nd, 3rd and 4th flash is depicted in Fig. 5. The spectrum after the 2nd flash differs noticeably from that of the 3rd and 4th flash, while the latter two are similar within the accuracy of the experiment. Particularly around the check point at 362 nm it is again evident that the absorption changes coupled with the $S_0 \rightarrow S_1$ transition are much smaller than those of the $S_1 \rightarrow S_2$ and $S_2 \rightarrow S_3$ transitions.

With the introduction of NH_2OH we have drastically reduced the strong mixing of the S-state transitions by shifting the $S_0 \rightarrow S_1$ transition to the front of the flash train, thereby preventing a mixing with the opposing jump coupled with the $S_3 \rightarrow S_0$ transition. Therefore, the spectra in Fig. 5 should present already characteristic features of the 'true' spectra. Nevertheless, the spectra are charged with a remaining 'soft' mixing. Fitting procedures for the patterns of Fig. 5 (for two examples see Fig. 4) yielded values for the misses of about $\alpha = 10\%$, on the average; i.e., higher than in the absence of NH_2OH (see Fig. 3). According to Hanssum and Renger [33] and Andréasson and Hanson [34], the S_2 and S_3 states deactivate much faster than the S_0 and S_1 states in the presence of hydroxylamine; i.e., the individual misses for the $S_1 \rightarrow S_2$ and $S_2 \rightarrow S_3$ transitions must be chosen greater than for the $S_3 \rightarrow S_0$ and $S_0 \rightarrow S_1$ transitions. Considering this, therefore in the presence of hydroxylamine, the corrected spectra of the $S_1 \rightarrow S_2 \rightarrow S_3$ transitions should be shifted by more than approx. 10% to higher absolute $\Delta\epsilon$ values, while the $S_0 \rightarrow S_1$ spectrum should change by less

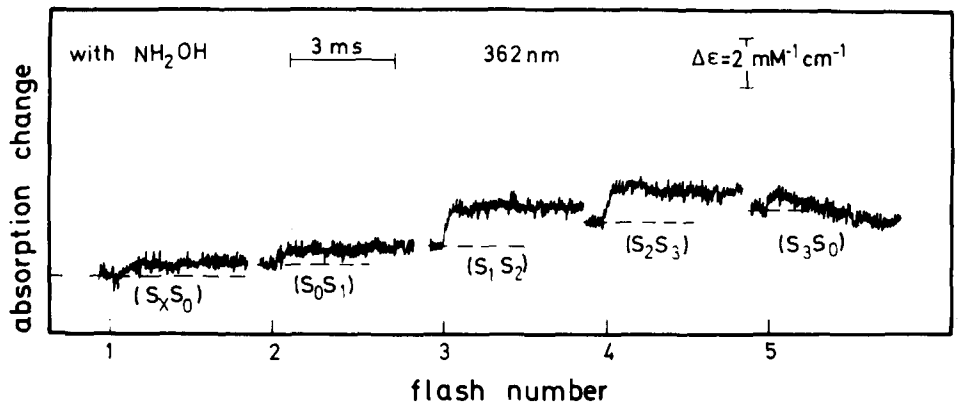

Fig. 6. Time-course of absorption changes at 362 nm in the presence of hydroxylamine as a function of flash number in the absence of an external acceptor. The time-courses are the difference of patterns in the presence of 24 μM NH_2OH and 1 mM NH_2OH. In this way one can eliminate contributions from the acceptor side (approx. 50% $Q_A^- Q_B^- \rightarrow Q_A Q^{2-}$ and approx. 50% $Q_A^- Q_B \rightarrow Q_A Q_B^-$ in each flash) so that mainly absorption changes of S-state transitions remain visible.

than 10%. This means that after fitting procedures the difference between the spectra of $S_0 \rightarrow S_1$ and the other two should even be greater than the difference in the 'soft' mixed spectra shown in Fig. 5.

Analysis of the kinetics in the presence of NH_2OH

As in the case without NH_2OH (Fig. 1), we also studied the kinetics in the presence of hydroxylamine. To observe the absorption changes of the S-state transitions in the ms range without being disturbed by the absorption changes of the acceptor side, we used the following technique: we subtracted the traces obtained in the presence of high concentrations of NH_2OH (2 mM) where the water oxidation is inhibited and NH_2OH donates electrons to PS II via D, from traces obtained in the presence of low concentrations of NH_2OH (24 μM), where the oxygen evolution is intact but the pattern is shifted by two flashes. Since no acceptor was used, the initial ratio of Q_B/Q_B^- is close to one which means that binary oscillations in both cases do not disturb (see Methods). The results are presented in Fig. 6. Since the $S_0 \rightarrow S_1$ transition is shifted to the 2nd flash and not masked by the mixing with an opposing $S_3 \rightarrow S_0$ transition, the amplitude can be roughly compared with those of the transitions in the 3rd and 4th flash. Again, one observes in the microsecond range at the check point 362 nm that the $S_0 \rightarrow S_1$ transition has a much smaller amplitude than $S_1 \rightarrow S_2$ and $S_2 \rightarrow S_3$.

Discussion

Despite the many difficulties in the determination of the 'true' difference spectra of the absorption changes coupled with the S-state transitions, it is at least an unambiguous result that the absorption changes coupled with the $S_1 \rightarrow S_2$ and $S_2 \rightarrow S_3$ transitions are similar, but that those of the $S_0 \rightarrow S_1$ transition are different from the latter; the 'spectrum' of $S_0 \rightarrow S_1$ is shifted to a shorter wavelength and characterized especially around 360 nm by much smaller $\Delta\varepsilon$ values (see Fig. 3, Table I and Fig. 5).

With this information the possible chemical groups involved in the accumulation process of the redox equivalents can be discussed. We assume that the $S_0 \rightarrow S_1$ transition is due to an Mn(II) → Mn(III) oxidation and the transitions $S_1 \rightarrow S_2$ and $S_2 \rightarrow S_3$ due to Mn(III) → Mn(IV) oxidations (see arguments below). With this assumption, the valence states of manganese in S_0, S_1, S_2 and S_3 states should be those outlined in Table III. The states are outlined for the cases where two and four Mn are engaged in the water oxidation. For the 4-Mn model, only one of several possibilities is discussed. With regard to the oxidizing equivalent created with the last transition from S_3 to the unstable (S_4), this may be, in the 2-Mn model, the oxidized form of the electron carrier D between Chl a_{II} and S (details see below). In the case of the 4-Mn model, in the last

transition from S_3 to S_4, D^+ might oxidize a third manganese. This remains 'invisible' with regard to transient absorption changes due to an immediate re-reduction together with the two oxidized Mn's in S_3. The fourth Mn might function only as stabilizer in a tetrameric Mn-cluster (see Table III). In the following arguments are presented which (a) support the valence state changes of Mn with the S_0–S_3 transitions and (b) allow conclusions as to the states of water coupled with the valence state changes of manganese.

The spectrum of the transition from Mn(II) to Mn(III) in certain in vitro complexes, e.g., in gluconate complexes, is shifted to shorter wavelengths compared to the Mn(III) to Mn(IV) change and characterized by smaller $\Delta\epsilon$ values [35–37]. This would be similar to the difference spectra shown in Fig. 5. Recently, isostructural Mn(II, III) and Mn(III, III) complexes with biologically relevant ligands have been synthesized [38]. The difference spectrum with a maximum at 303 nm is close to that of Fig. 5 for the $S_0 \rightarrow S_1$ transition. The $\Delta\epsilon$ values are also comparable. It must be pointed out that the states responsible for the absorption of the individual S states should depend – besides the possible valence states of manganese – more or less also on the different states of the ligating water and on the presence of surplus charges (see Table III). In this discussion it is, however, assumed that the dependence on the valence states is the dominating factor.

After dark adaptation, S_1 is the major stable state of S. According to Table III, in S_1 only Mn(III) states are present or dominating. In some in vitro complexes Mn(II) is unstable in the presence of oxygen [39,40]; on the other hand, Mn(IV) should be unstable in the neighbourhood of intrinsic donors. Therefore, the Mn(III) state in S_1 may explain its stabilization in the dark. (For a further stabilization of S_1 through a special binding of H^+, see the final paragraph of this section.)

The multi-line EPR signal [41–45] of manganese can be explained by the presence of Mn(III)–Mn (IV) valence states in S_2. This corresponds to Table III, in which such a manganese redox-level constellation is present in S_2.

In the presence of NH_2OH (low concentration) the 'deactivation' of S_2 and S_3 is much faster than that of S_1 [33,34]. This demonstrates with regard to the reactivity again the difference of S_1 from S_2

TABLE III

STOICHIOMETRY AND STATES OF DIFFERENT EVENTS IN THE TURNOVER OF THE WATER-SPLITTING ENZYME SYSTEM, S

S-state transitions	S_0	$\rightarrow S_1$	$\rightarrow S_2$	$\rightarrow S_3$	$\rightarrow (S_4) \rightarrow$	S_0
Absorbed quanta $h\nu_{II}$	1	1	1	1		
Electron extraction Chl $a_{II}^+ \leftarrow e^- \ldots S_n$	1	1	1	1		
Changes of positive surplus charges	0	1	0	−1		
Intrinsic H^+ release	1	0	1	2		
Surplus charge	○	○	⊕	⊕		○
Possible states of water	OH^- OH^-	OH^- O^-	OH^- O^-	O^- O^-	$-O_2$ $+2H_2O$	OH^- OH^-
Possible states of Mn if two manganese are engaged in water oxidation	Mn^{2+} Mn^{3+}	Mn^{3+} Mn^{3+}	Mn^{3+} Mn^{4+}	Mn^{4+} Mn^{4+}	Mn^{4+} Mn^{4+} D^+	Mn^{2+} Mn^{3+}
Possible states of Mn if four manganese are engaged in water oxidation	Mn^{2+} Mn^{3+} Mn^{2+} Mn^{2+}	Mn^{3+} Mn^{3+} Mn^{2+} Mn^{2+}	Mn^{3+} Mn^{4+} Mn^{2+} Mn^{2+}	Mn^{4+} Mn^{4+} Mn^{2+} Mn^{2+}	Mn^{4+} Mn^{4+} Mn^{3+} Mn^{2+}	Mn^{2+} Mn^{3+} Mn^{2+} Mn^{2+}

and S_3. This can be understood according to Table III by a fast Mn(IV) reduction in S_2 and S_3 and a slow Mn(III) reduction in S_1 and S_0, lastly ending in S_x (see the next paragraph).

Reductants like NH_2OH but also NH_2NH_2 and H_2O_2 shift the S-states in the dark backwards by two units to an unknown state, S_x. This is documented by the fact that in the presence of these reductants, after the 1st flash not S_2 (see Eqn. 1) but S_0 is created (see Results). Different mechanistic models are discussed for this effect. According to Radmer and Ollinger [46], the reaction sequence for NH_2OH should be:

(a) $S_1 + 2\,NH_2OH \xrightarrow{dark} S_0(NH_2OH) + \frac{1}{2}\,N_2 + H_3O^+$

$S_0(NH_2OH) \xrightarrow{1st\ flash} S_1(NH_2OH) \xrightarrow[water]{}$

$\xrightarrow[water]{} S_0(water) + \frac{1}{2}\,N_2 + H_3O^+$

The suggestion in Refs. 47 and 48 is the binding of four NH_2OH:

(b) $S_1 + 4\,NH_2OH \xrightarrow{dark} S_1^* \cdot 4\,NH_2OH$

$S_1^* \cdot 4\,NH_2OH \xrightarrow{1st\ flash} [S_1^* \cdot 4\,NH_2OH]_{ox} \xrightarrow[water]{}$

$\xrightarrow[water]{} S_0(2\,OH^-) + [4\,NH_2OH]^{2+} + 2\,H^+$

Our results – see below and Ref. 20 – may indicate the following sequence:

(c) $S_1(O^{2-}\,OH^-) + 2\,NH_2OH$

$\xrightarrow{dark} S_x(2\,H_2O) + N_2 + H_2O + OH^-$

$S_x(2\,H_2O) \xrightarrow{1st\ flash} S_0(2\,OH^-) + 2\,H^+$

S_x should represent a state 'over-reduced' through NH_2OH by one unit with regard to S_0. In models (a) and (b) an oxidation of NH_2OH should occur in the 1st flash but not in model (c). In (a), probably also in (b), this oxidation should be accompanied by an N_2 evolution. N_2 evolution in the 1st flash has been measured according to Radmer's results [46]. But it was outlined in the Discussion in Ref. 20 that the measured N_2 yield in Ref. 46 is 20-times too low to support the mechanism in (a). According to (a), one H^+ should be released after the 1st flash, but the release of two H^+ has been measured in Refs. 20 and 48 (see paragraph on page 465, beginning with 'We have shown by ...').

In a similar 'two-unit shift' experiment with H_2O_2 (instead of NH_2OH) in case of (a) and (b) oxidation of H_2O_2 should take place after the 1st flash, i.e., O_2 instead of N_2 evolution. This has been checked and O_2 evolution was not observed [49]. Therefore, in the case of H_2O_2 it is very likely to assume mechanism (c); i.e., that H_2O_2 reduces S_1 to S_0 and, in a further step, S_0 to an over-reduced state, S_x. This makes the existence of S_x, also for NH_2OH and NH_2NH_2, probable. Otherwise, one has to accept for H_2O_2, on one hand, and NH_2OH and NH_2NH_2, on the other hand, two different mechanisms for the same phenomenon: backwards shift from S_1 by two units.

A consequence of the existence of a state S_x, reduced through NH_2OH by one more unit with regard to S_0, is that the first two flashes should induce practically the same spectrum, because according to the valence state of S_0 (see Table III) an Mn(II) → Mn(III) transition must take place twice: $S_x \xrightarrow{1st\ flash} S_0 \xrightarrow{2nd\ flash} S_1$. The asterisks in Fig. 5 show the absorption changes after the 1st flash. Although not comparable to the absorption change after the 2nd flash, the changes of the 1st flash all have positive absorptions in the range of 270–370 nm. Deviations may be due to that part of particles which was deactivated through the addition of NH_2OH (approx. 25%, see Materials) but can still perform on turnover with abnormal changes ('first flash event', see Introduction). According to model (a) in the previous paragraph, the difference spectrum after the 1st flash should be practically zero, because in this model $S_0(NH_2OH)$ changes to S_0(water). This is in contrast to the positive absorption changes of the 1st flash depicted in Fig. 5, if one assumes that the absorption changes due to the change of the ligands in S_0 from NH_2OH to water are negligible. According to model (b), mainly an inverse, i.e., negative, spectrum should appear because in (b) after the 1st flash, S_1 is moved to S_0. This is also in disagreement with the positive absorption changes in Fig. 5. Therefore, the 1st flash result in Fig. 1 supports model (c) and, thereby, the existence of a state S_x. The formation of S_x through

NH_2OH, evaluated in this paragraph and the previous one, is a very helpful result, because if we know the chemical products of the action of NH_2OH, i.e., especially the composition of S_x with regard to manganese, then we also know the S_0 state and, as a consequence, all other states.

In vitro experiments show that NH_2OH reduces Mn complexes of higher valence states up to Mn(II) [50]. Recently, Wieghardt et al. have shown (unpublished results) that through NH_2OH the synthesized binuclear complexes of Mn(III) [51] as well as those of Mn(III)-Mn(IV) [52] are reduced to Mn(II), whereby the oxidation of NH_2OH is accompanied by N_2 evolution. If also in vivo the reduction through NH_2OH ends fully in Mn(II) states, then S_x must be composed of Mn(II)'s only. Consequently, the S_0 state – oxidized by one unit more with regard to S_x – must be characterized by Mn(II) states plus one Mn(III). This is in accordance with the valence states in the 2-Mn as well as the 4-Mn model of Table III. Starting with S_0 state, 'calibrated' in such a way, as a consequence the valence states in S_1–S_3 are also known; they are identical with those already outlined in Table III but founded by other arguments (see above).

We have shown by electrochromism that in the presence of NH_2OH after the 1st flash a negative surplus charge is created with the formation of S_0 after the 1st flash [20]. This means that with the electron extraction from S_x and the formation of S_0 two H^+ must have been released. This has also been observed by pH measurements [48]. If after the 1st flash the transition S_x (2 Mn(II)) → S_0(Mn(II), Mn(III)) occurs (see above), then these protons originate very probably from water bound in S_x. This is plausible because if hydroxylamine is bound in S_x in the first coordination sphere of manganese, it would have been oxidized after the 1st flash together with N_2 evolution. This has, however, not been observed (see above). Since 4 H^+ are released in the reaction sequence from S_x to S_3 (2 H^+ with the transition $S_x \rightarrow S_0$, 1 H^+ with $S_0 \rightarrow S_1$, 1 H^+ with $S_2 \rightarrow S_3$), this is possible if S_x is loaded with two undissociated H_2O molecules, i.e., S_x (2 H_2O). Consequently, water must be present in S_0 in the dissociated form, that is, S_0(2 OH^-) [20]. Two OH^- in S_0 was evaluated through ESR analysis already in Ref. 53 and discussed as a possibility in Ref. 48.

The changes of surplus charges with the S-state transition were observed by analysis of the Chl a_{II}^+ re-reduction kinetics [10] as well as electrochromism [28,54]. From the observed patter of changes of charges the stoichiometry of the intrinsic H^+ release for all 3 states is available (see Table III). Starting with S_0(2 OH^-) the possible states of water in the other S states are consequently known (see Table III).

The H^+ release in the cycle of water cleavage should be a subsequent event of the electron transfer and not vice versa. This is in accordance with the transfer times outlined in Table II; these values are all below the times measured for the external H^+ release in Ref. 55. The values measured in Refs. 16 and 32 are for the $S_2 \rightarrow S_3$ transition longer than those for the H^+ release. This calls for complicated explanations [55].

Since with the transition from S_0 to S_3 all electrons are extracted from Mn, an essential feature of this result is that water is not oxidized in the transition from S_0 to S_3. This statement was outlined already in Ref. 19 and recently by Radmer [56] who showed that ^{16}O water added to a suspension of PS II particles which was illuminated before by two flashes in labeled $H_2{}^{18}O$ (brought the system mainly to state S_3) was able to evolve $^{16}O_2$ on the following 3rd flash ($S_3 \xrightarrow{(S_4)} S_0$ transition). Similar results were obtained by Bader et al. [57].

The main feature of the results in Figs. 1–6 is that the $S_0 \rightarrow S_1$ transitions are different from $S_1 \rightarrow S_2 \rightarrow S_0$. These results together with the arguments discussed in all the previous paragraphs of this section support the statement that $S_0 \rightarrow S_1$ may be due to an Mn(II) → Mn(III) transition and $S_1 \rightarrow S_2 \rightarrow S_3$ due to an Mn(III) → Mn(IV) one. The arguments exhibit also the specific Mn compositions in the different S states. A 2-Mn as well as a 4-Mn model is discussed. That all 4 Mn localized in Photosystem II are engaged in water oxidation was argued by De Paula et al. [61], on the basis of the non-Curie behavior of the EPR multiline signal of manganese. However, recently Pace R.J., Smith, P.J., Bramley, R. and Stehlik, D. (unpublished results) have investigated the complete saturation behaviour of the signal, giving evidence that the EPR signal exhibits Curie be-

haviour. Then a coupling of the anti-ferromagnetic coupled Mn dimer to other paramagnetic manganese species resulting in a 4-Mn complex is no longer necessary; i.e., a 2-Mn model is not excluded. The argument by Dekker et al. [19] for a 4-Mn model was based on three equal changes (Mn(III) → Mn(IV)) with the $S_0 \rightarrow S_1 \rightarrow S_2 \rightarrow S_3$ transition. If they are no longer relevant (see this work), then, also from this point of view, a 2-Mn model is open for discussion. Preferring the simplest model, we have outlined the 2-Mn model in more detail.

For the case of a 2-Mn model we suggest as possible configurations of manganese and water in the different S states those outlined in Scheme II. Mn is probably stabilized on the polypeptide framework by ligating atoms on one hand and water as ligand on the other hand. Principally, after every electron extraction from S also a proton should be removed from S so that the total charge does not change. A stable step where no proton release takes place is the $S_1 \rightarrow S_2$ transition, whereby consequently also a positive surplus charge formation ⊕ takes place in S_2 and S_3 (Table III). This charge may be partially neutralized by a chloride ion which may enter the outer coordination sphere of the manganese [58,59]. One plausible reason for the failure of a proton release could be that the proton is particularly stabilized through intramolecular hydrogen bonds to two oxoatoms as outlined in Scheme II. This configuration is supported by analogous constellations. On one hand we have shown that acetate can inhibit O_2-evolution activity reversibly [59], probably by exchange in S_1 against the bound water. On the other hand, Wieghardt et al. [52,60] have demonstrated that on oxo-Mn-complexes acetate can replace the two oxo groups in a very uncomplicated manner by exchanging them through the OCO-group with minor movements in the atomic distances. (This H^+ stabilization in S_1 may be a further reason for the stabilization of S_1 in the dark, see the paragraph on page 463, beginning with 'After dark adaptation ...'.) With respect to the S_4 state it may be that already the electrostatic field of D^+ is the actual promotor giving rise to the electron transfer from the oxo-atoms to the 2 Mn(IV). A 2-Mn(III)-peroxo-intermediate (see dotted circle) may be considered on the way to the 2-Mn(II) and O=O formation. A subsequent Mn(II)-Mn(III) formation through D^+ reduction, uptake of 2 H_2O and release of 2 H^+ ends up in

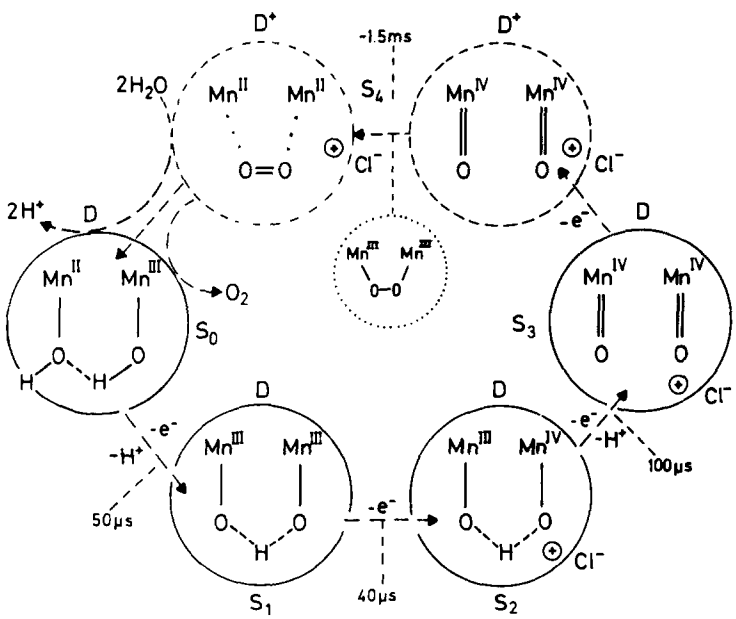

Scheme II. Possible states and configurations of water and manganese in the 2-Mn model of the water cleavage cycle in photosynthesis (for details, see text). The times shown indicate the electron transfer times.

S_0 (see Scheme II). The rate-limiting step of the cycle of water cleavage takes approx. 1.2 ms [12]. This is probably identical with the 1.5 ms time of the absorption decrease and reduction of manganese, in the transition $S_3 \rightarrow S_0$ (see Table II). This step should be located between S_3 and S_4 because a manganese reduction takes place according to Scheme II only in this transition, not between S_4 and S_0.

Conclusions

Our results shown in Table III and Scheme II do not support any of the models proposed in other works. They are only in accordance with our alternative interpretation at the end of Ref. 20. The absence of absorption changes in the ultraviolet in the $S_0 \rightarrow S_1$ and $S_2 \rightarrow S_3$ transitions as outlined by Velthuys [14] and Lavergne [15] has not been confirmed by Dekker et al. [19] and our work. According to Dekker et al., in all transitions from S_0 to S_3 the same event takes place (Mn(III) $\rightarrow$ Mn(IV)) on at least three Mn atoms. In our results the transition $S_0 \rightarrow S_1$ differs from $S_1 \rightarrow S_2$ and $S_2 \rightarrow S_3$.

Regardless of the methodic differences (see below), there is one point in Dekker's results which remains incomprehensible: the spectra of Dekker et al. contain a contribution from a binary oscillation of absorption changes of plastoquinone at the acceptor side. They subtracted, of course, this binary oscillation from the overall spectra. The remaining spectra do not result in three times the same spectra for $S_0 \rightarrow S_3$. This is only the case when they label the acceptor side contribution with factors between 0.71 and 1.19. These correction devices remain unexplained and thereby cast doubt on the conclusions.

Apart from this remark one should discuss the differences on the basis of the methods used. Firstly, the binary oscillation problem was solved in this work especially through the use of SiMo and high DCBQ concentrations, respectively (see Methods). Secondly, the problem of the mixing of the S states with increasing flash numbers was tentatively solved by deconvolution of the overlapping spectra through calculations based on the S_0/S_1 ratio and α and β values (see Introduction). In this respect we have done the same fitting procedures as all other authors active in this field. According to our results we calculated from $\Delta\epsilon_{irrev}$ at the check point at 362 nm for $S_0 \rightarrow S_1$ a different $\Delta\epsilon$ value as that for $S_1 \rightarrow S_2$ and $S_2 \rightarrow S_3$ (Fig. 3, center and Table I) in contrast to Dekker et al. This discrepancy is not astonishing because it was shown that the fitting procedure alone is not unambiguous [20]. Particularly, since all authors in this field detected practically no stable absorption change in the whole ultraviolet region after the 4th flash, it does not feel right that by deconvolution from 'nothing' the spectrum of the corresponding $S_0 \rightarrow S_1$ transition should be available. For this reason, besides the fitting procedures to the stable levels, the result was checked by additional methods. Thirdly, we analyzed the transient levels of $\Delta\epsilon_{max}$ attained in the time range up to 200 μs where neither the mixing through the contribution of the $S_0 \rightarrow S_3$ transition nor the binary oscillations are effective, since they only take place in the millisecond time range. At the 362 nm check point it was found again that the $S_0 \rightarrow S_1$ transition is different from the $S_1 \rightarrow S_2$ and $S_2 \rightarrow S_3$ transitions (Fig. 3 below, and Table I). Fourthly, besides this method the concealment of the $S_0 \rightarrow S_1$ transition by the opposite $S_3 \rightarrow S_0$ transition was eliminated by shifting the S states two units backwards by the addition of small amounts of NH_2OH. Again, it resulted that the $S_0 \rightarrow S_1$ transition is different from $S_1 \rightarrow S_2$ and $S_2 \rightarrow S_3$ not only in the range of 360 nm but practically at all other wavelengths between 260 and 400 nm (Fig. 5). Lastly, the transient amplitudes, $\Delta\epsilon_{max}$, attained after a flash in the 200 μs range were also analyzed in the presence of hydroxylamine. At the check point of 362 nm, again the $S_0 \rightarrow S_1$ transition is different from the other two transitions (Fig. 6).

This work demonstrates by the use of five different methods the same result. A methodological advance was the use of a highly purified simple Photosystem-II complex of high optical quality isolated from the cyanobacterium *Synechococcus* sp. We believe that by the extensive changes of the conditions in this work, in particular through the use of NH_2OH and by elimination of the binary oscillation through the use of SiMo and DCBQ, respectively, as acceptors, the ambiguities inherent in the procedure of fittings and subtraction of

binary oscillations have been circumvented. Table III and Scheme II give a convenient interpretation of our results in terms of the possible states of water and manganese.

Acknowledgements

The financial support of the Deutsche Forschungsgemeinschaft (Sonderforschungsbereich 312, Teilprojekt A3) is gratefully acknowledged. We wish to thank Dr. K. Brettel, Dr. J.P. Dekker and Dr. E. Schlodder for reading the manuscript and for comments. We thank Ms. D. DiFiore and Ms. I. Geisenheimer for their excellent technical assistance.

References

1 Döring, G., Stiehl, H.H. and Witt, H.T. (1967) Z. Naturforsch. 22b, 639–644
2 Döring, G., Renger, G., Vater, J. and Witt, H.T. (1969) Z. Naturforsch. 24b, 1139–1143
3 Stiehl, H.H. and Witt, H.T. (1968) Z. Naturforsch. 23b, 220–224
4 Stiehl, H.H. and Witt, H.T. (1969) Z. Naturforsch. 24b, 1588–1598
5 Junge, W. and Witt, H.T. (1968) Z. Naturforsch. 23b, 244–254
6 Witt, H.T. (1979) Biochim. Biophys. Acta 505, 355–427
7 Bouges-Bocquet, B. (1973) Biochim. Biophys. Acta 333, 85–94
8 Kok, B. (1957) Acta Bot. Neerl. 6, 316–336
9 Tiemann, R., Renger, G., Gräber, P. and Witt, H.T. (1979) Biochim. Biophys. Acta 546, 498–519
10 Brettel, K., Schlodder, E. and Witt, H.T. (1984) Biochim. Biophys. Acta 766, 403–415
11 Blankenship, R.E., Babcock, G.T., Warden, J.T. and Sauer, K. (1975) FEBS Lett. 51, 287–293
12 Joliot, P., Barbieri, G., Chabaud, R. (1969) Photochem. Photobiol. 10, 309–329
13 Kok, B., Forbush, B., McGloin, M. (1970) Photochem. Photobiol. 11, 457–475
14 Velthuys, B.R. (1981) in Photosynthesis II (Akoyunoglou, ed.), pp. 75–85, Balaban International Science Services, Philadelphia, PA
15 Lavergne, J. (1986) Photochem. Photobiol. 43, 311–316
16 Renger, G. and Weiss, W. (1986) Biochem. Soc. Trans. 14, 17–20
17 Renger, G. and Weiss, W. (1986) Biochim. Biophys. Acta 850, 184–196
18 Renger, G., Hansum, B. and Weiss, W. (1987) in Progress in Photosynthesis Research (Biggins, J., ed.), Vol. I, pp. 541–544, Martinus Nijhoff, Dordrecht
19 Dekker, J.P., Van Gorkom, H.J., Wensink, J. and Ouwehand, L. (1984) Biochim. Biophys. Acta 767, 1–9
20 Saygin, Ö. and Witt, H.T. (1985) Photobiochem. Photobiophys. 10, 71–82
21 Saygin, Ö. and Witt, H.T. (1987) in Progress in Photosynthesis Research (Biggins, J., ed.), Vol. I, pp. 537–540, Martinus Nijhoff, Dordrecht
22 Bowes, J.M. and Crofts, A.R. (1980) Biochim. Biophys. Acta 590, 373–384
23 Mathis, P. and Havemann, J. (1977) Biochim. Biophys. Acta 461, 167–181
24 Schatz, G.H. and Van Gorkom, H.J. (1985) Biochim. Biophys. Acta 810, 283–294
25 Bouges, B. (1971) Biochim. Biophys. Acta 234, 103–112
26 Schatz, G.H. and Witt, H.T. (1984) Photobiochem. Photobiophys. 7, 1–14 and 77–89
27 Rögner, M., Dekker, J.P., Boekema, E.J. and Witt, H.T. (1987) FEBS Lett. 219, 207–211
28 Saygin, Ö. and Witt, H.T. (1984) FEBS Lett. 176, 83–87
29 Diner, B.A. and De Vitry, C. (1984) in Advances in Photosynthesis Research (Sybesma, C., ed.), Vol. I, pp. 407–411, Martinus Nijhoff/Dr. W. Junk Publishers, Dordrecht
30 Dekker, J.P., van Gorkom, H.J., Brok, M. and Ouwehand, L. (1984) Biochim. Biophys. Acta 764, 301–309
31 Weiss, W. and Renger, G. (1986) Biochim. Biophys. Acta 850, 173–183
32 Dekker, J.P., Plijter, J.J., Ouwehand, L. and Van Gorkom, H.J. (1984) Biochim. Biophys. Acta 767, 176–179
33 Hansum, B. and Renger, G. (1985) Biochim. Biophys. Acta 810, 225–234
34 Andreasson, L.-E. and Hansson, Ö. (1987) in Progress in Photosynthesis Research (Biggins, J., ed.), Vol. I, pp. 503–510, Martinus Nijhoff, Dordrecht
35 Bodini, M.E., Willis, L.A., Riechel, T.L. and Sawyer, D.T. (1976) Inorg. Chem. 15, 1538–1543
36 Cartledge, G.H. and Ericks, W.P. (1936) J. Am. Chem. Soc. 58, 2065–2069
37 Cartledge, G.H. and Ericks, W.P. (1936) J. Am. Chem. Soc. 58, 2069–2072
38 Vincent, J.B. and Christou, G. (1986) FEBS Lett. 207, 250–252
39 Lawrence, G.D. and Sawyer, D.T. (1978) Coord. Chem. Rev. 27, 173–193
40 Magers, K.D., Smith, C.G. and Sawyer, D.T. (1978) J. Am. Chem. Soc. 100, 989–991
41 Dismukes, G.C. and Siderer, Y. (1981) Proc. Natl. Acad. Sci. USA 78, 274–278
42 Hansson, Ö. and Andreasson, L.-E. (1982) Biochim. Biophys. Acta 679, 261–268
43 Brudvig, G.W., Casey, J.L. and Sauer, K. (1983) Biochim. Biophys. Acta 723, 366–371
44 Casey, J.L. and Sauer, K. (1984) Biochim. Biophys. Acta 767, 21–28
45 Zimmermann, J.L. and Rutherford, A.W. (1984) Biochim. Biophys. Acta 767, 160–167
46 Radmer, R. and Ollinger, O. (1982) FEBS Lett. 144, 162–166
47 Förster, V. and Junge, W. (1985) FEBS Lett. 186, 153–157
48 Förster, V. and Junge, W. (1985) Photochem. Photobiol. 41, 191–194

49 Velthuys, B.R. and Kok, B. (1978) Biochim. Biophys. Acta 211–221
50 Wieghardt, K. (1984) in Advances in Inorganic and Bioinorganic Mechanisms (Skykes, A.G., ed.), Vol. 3, pp. 213–273, Academic Press, New York
51 Wieghardt, K., Bossek, U., Ventur, D. and Weiss, J. (1985) J. Chem. Soc. Chem. Commun. 347–349
52 Wieghardt, K., Bossek, U., Bonvoisin, J., Beauvillain, P., Girerd, J.-J., Nuber, B., Weiss, J. and Heinze, J. (1986) Angew. Chem. 98, 1026–1027
53 Andréasson, L.-E., Hansson, Ö. and Vänngard, T. (1983) Chem. Scr. 21, 71–74
54 Saygin, Ö. and Witt, H.T. (1985) FEBS Lett. 187, 224–226
55 Förster, V. and Junge, W., (1986) Photosynth. Res. 9, 197–210
56 Radmer, R. and Ollinger, O. (1986) FEBS Lett. 195, 285–289
57 Bader, K.P., Thibault, P. and Schmid, G.H. (1987) in Progress in Photosynthesis Research (Biggins, J., ed.), Vol. I, pp. 549–556, Martinus Nijhoff, Dordrecht
58 Preston, C. and Pace, R.J. (1985) Biochim. Biophys. Acta 810, 388–391
59 Saygin, Ö., Gerken, S., Meyer, B. and Witt, H.T. (1986) Photosynth. Res. 9, 71–78
60 Wieghardt, K., Bossek, U., Zsolnai, L., Huttner, G., Blondin, G., Girerd, J.-J. and Babonneau, F. (1986) J. Chem. Soc. Chem. Commun., in the press
61 De Paula, J.C., Beck, W.F. and Brudvig, G.W. (1986) J. Am. Chem. Soc. 108, 4002–4009